Intra- and Inter-Islet Synchronization of Metabolically Driven Insulin Secretion

Morten Gram Pedersen,* Richard Bertram,† and Arthur Sherman‡
*Department of Mathematics, Technical University of Denmark, Kgs. Lyngby, Denmark; †Department of Mathematics and Institute of Molecular Biophysics, Florida State University, Tallahassee, Florida; and ‡Laboratory of Biological Modeling, National Institute of Diabetes and Digestive and Kidney Diseases, National Institutes of Health, Bethesda, Maryland

ABSTRACT Insulin secretion from pancreatic β-cells is pulsatile with a period of 5–10 min and is believed to be responsible for plasma insulin oscillations with similar frequency. To observe an overall oscillatory insulin profile it is necessary that the insulin secretion from individual β-cells is synchronized within islets, and that the population of islets is also synchronized. We have recently developed a model in which pulsatile insulin secretion is produced as a result of calcium-driven electrical oscillations in combination with oscillations in glycolysis. We use this model to investigate possible mechanisms for intra-islet and inter-islet synchronization. We show that electrical coupling is sufficient to synchronize both electrical bursting activity and metabolic oscillations. We also demonstrate that islets can synchronize by mutually entraining each other by their effects on a simple model "liver," which responds to the level of insulin secretion by adjusting the blood glucose concentration in an appropriate way. Since all islets are exposed to the blood, the distributed islet-liver system can synchronize the individual islet insulin oscillations. Thus, we demonstrate how intra-islet and inter-islet synchronization of insulin oscillations may be achieved.

INTRODUCTION

Insulin secretion from pancreatic β-cells, located in the islets of Langerhans, is pulsatile with a period of 5–10 min and is believed to be responsible for in vivo pulsatility with similar frequency (1–3). It has been suggested that this is due to oscillations in glycolysis mediated by the allosteric enzyme phosphofructokinase (PFK), resulting in rhythmic activity of ATP-dependent potassium channels (K(ATP)-channels) (3–6). Insulin pulsatility is impaired in diabetic humans (7), their relatives (8,9) and in animal models such as ob/ob mice (10) and ZDF rats (2). Moreover, target tissues are more sensitive to pulsatile insulin levels than to constant levels (11–14). Hence, understanding the mechanisms underlying pulsatile insulin secretion is important for a potential medical treatment of diabetes.

The link between metabolism and Ca^{2+} influx leading to insulin secretion is provided by the electrical activity of the β-cells, which has a characteristic behavior known as ''bursting.'' A burst consists of an active phase of spiking followed by a silent phase of hyperpolarization. During the active phase Ca^{2+} enters the cell through voltage-gated calcium channels leading to an elevated cytosolic Ca^{2+} concentration and the consequent release of insulin. During the silent phase Ca^{2+} is cleared by Ca^{2+} ATPases. When the glucose concentration is increased, increasing the strength of the metabolic stimulus, K(ATP)-channels close and the plateau fraction increases, i.e., the active phases become longer compared to the silent phases. In this way, glucose increases the average Ca^{2+} concentration, which increases the rate of insulin release (15). The period of this ''simple'' bursting is often tens of seconds.

Another form of bursting called ''compound bursting'' consists of clusters or episodes of bursts followed by long silent phases (6). Compound bursting has often been observed in electrical and calcium recordings from β-cells in islets (6,16–18). The period of a compound burst is several minutes, considerably longer than a single simple burst. It has been suggested that compound bursts are responsible for pulsatile insulin secretion (6).

In Bertram et al. (6) a potential mechanism for compound bursting was described. In this model, the glycolytic subsystem has the ability to oscillate due to positive product feedback onto the glycolytic enzyme PFK. The oscillatory glycolysis leads to oscillations in ATP production which lead to periodic activity of K(ATP)-channels. This slow rhythm interacts with the faster activity-dependent Ca^{2+} rhythm that drives simple bursting, producing episodes of bursting followed by long silent phases. In addition to compound bursting, oscillations in glycolysis were shown to have other possible effects. These include production of a very slow form of bursting driven purely by glycolysis (''glycolytic bursting''), and a periodic variation in the plateau fraction (''accordion bursting''). These various forms of bursting have in common a slow modulation of the intracellular calcium concentration, and consequent pulsatile insulin secretion.

To observe an overall oscillatory insulin profile it is necessary that the insulin secretion from individual β-cells is synchronized within islets (intra-islet synchronization), and that the population of islets is also synchronized (inter-islet synchronization). If the cells or islets were not synchronized we would observe a flat, averaged signal even though the single cells and islets released insulin in pulses. This raises the questions

Submitted November 8, 2004, and accepted for publication April 6, 2005.

Address reprint requests to Arthur Sherman, Tel.: 301-496-4325; E-mail: asherman@nih.gov.

© 2005 by the Biophysical Society

0006-3495/05/07/107/13 $2.00

doi: 10.1529/biophysj.104.055681

of how metabolic oscillations are synchronized within and among islets. These questions are the focus of this report.

Insulin secretion from the isolated pancreas is pulsatile (19,20), and this has lead to the hypothesis that an intrapancreatic neural pacemaker may be responsible for inducing periodic insulin release from the population of islets (3,19,21). However, pulsatile insulin secretion has been observed in individual β-cells (22) and islets (1,2,23), demonstrating that such a pacemaker has, at most, a synchronizing function. It has also been shown that groups of islets (2,24) and pieces of pancreas containing electrically silent ganglia (25) exhibit oscillatory release of the hormone. Hence, there must be additional synchronizing mechanisms.

An alternate synchronization mechanism has been postulated based on data showing that plasma glucose levels fluctuate on the timescale of pulsatile insulin release (26–30). According to this mechanism, classical glucose/insulin feedback pathways account for the synchronization of the islets (2,3,20,21). We stress that this is a synchronization mechanism only, since the ability to secrete in 5–10 min pulses resides within the individual cells and islets. This is in contrast to the slower ultradian oscillations of insulin which have periods of hours. Here the feedback between the islets and the liver is believed to create the oscillations, not just synchronize those that are already present in the islets (31).

The possibility that oscillations in glucose feed back onto the 5–10 min insulin pulses is supported by the following facts. It has been shown that pulsatile insulin secretion can be entrained by a periodic glucose stimulus in healthy rats (1,2) as well as in healthy humans (29,30). Moreover, slow NAD(P)H, Ca^{2+}, and mitochondrial membrane potential oscillations, which are thought to underlie pulsatile insulin release, can be entrained in mouse islets (32). The entrainment is impaired in ZDF rats (2) and diabetic humans (29,33), pointing to a possibly crucial mechanism for normal overall pulsatility. Similar results have been obtained for entrainment of the slower ultradian oscillations (31,34).

Not all data support the glucose/insulin feedback mechanism for synchronization. For example, pulsatile secretion has been observed even when the glucose concentration was held constant. This has been observed in vitro for the perfused pancreas (19) as well as in vivo when plasma glucose was clamped (35). Our aim here is not to reconcile all of the in vitro and in vivo data, but rather to test the plausibility that insulin oscillations can be produced and coordinated in the absence of an intrapancreatic neural pacemaker.

Using the model of Bertram et al. (6), we investigate possible mechanisms for intra-islet and inter-islet synchronization. We show that, surprisingly, electrical coupling is sufficient to synchronize both electrical bursting activity and metabolic oscillations. We also demonstrate that inter-islet synchronization is possible through the glucose/insulin feedback mechanism described above, here modeled by the interaction of β-cells with a ''liver.'' The simple model liver responds to the level of insulin secretion by adjusting the external glucose concentration in an appropriate way. Furthermore, we show that some degree of pulsatile secretion from groups of islets can be expected even when glucose is kept constant. Thus, intra-islet and inter-islet synchronization are possible for a model β-cell in which pulsatile insulin secretion is produced through compound bursts involving glycolytic oscillations.

MATERIALS AND METHODS

Modeling

We use the model developed by Bertram et al. (6), which combines a model for electrical and Ca^{2+} dynamics from Bertram and Sherman (36) with a model for glycolysis that is modified from Smolen (37). To this model we add a first-order equation for insulin secretion. The link between glycolysis and the electrical/ Ca^{2+} component of the model is provided by the adenine nucleotides adenosine monophosphate (AMP), adenosine diphosphate (ADP), and adenosine triphosphate (ATP) (3,4,6). The model is summarized in Fig. 1.

The glycolytic component of the model (*left side* of Fig. 1) is modified from an earlier model for glycolytic oscillations in muscle extracts (37). The key player in glycolysis for the production of oscillations is the allosteric enzyme phosphofructokinase (PFK). This is activated by its product fructose 1-6-bisphosphate (FBP) and by adenosine monophosphate, and inhibited by ATP. The main difference from the recent model by Westermark and Lansner (38) is that their model does not include feedback of ATP and AMP onto PFK.

The glycolysis model consists of equations for intracellular glucose (G_i), glucose 6-phosphate (G6P) and FBP,

$$\frac{dG_i}{dt} = J_{glut} - J_{gk}, \tag{1}$$

$$\frac{dG6P}{dt} = \kappa(J_{gk} - J_{PFK}), \tag{2}$$

$$\frac{dFBP}{dt} = \kappa(J_{PFK} - \frac{1}{2}J_{GPDH}). \tag{3}$$

The concentrations of G6P and fructose 6-phosphate (F6P) are assumed to be in equilibrium through rapid catalytic activity of the enzyme phosphoglucose isomerase. They satisfy the equilibrium relation F6P = 0.3 G6P.

The parameter $\kappa = 0.005$ (in 2–3) converts milliseconds to seconds and increases the frequency of glycolytic oscillations by a factor of 5 with respect to the earlier Smolen model (37). J_{glut} is the rate of the GLUT-2 facilitated glucose transporter (39),

$$J_{glut} = V_{glut}\frac{(G_e - G_i)K_{glut}}{(K_{glut} + G_e)(K_{glut} + G_i)}, \tag{4}$$

where G_e is the extracellular glucose concentration, V_{glut} is the maximal rate, and K_{glut} is a constant. The value J_{gk} is the glucokinase reaction rate, which is described by a Hill function of G_i (40), where it is assumed that the reaction is irreversible:

$$J_{gk} = V_{gk}\frac{G_i^{n_{gk}}}{K_{gk}^{n_{gk}} + G_i^{n_{gk}}}. \tag{5}$$

Furthermore,

$$J_{GPDH} = 0.2\sqrt{\frac{FBP}{1\,\mu M}}\,\mu M s^{-1} \tag{6}$$

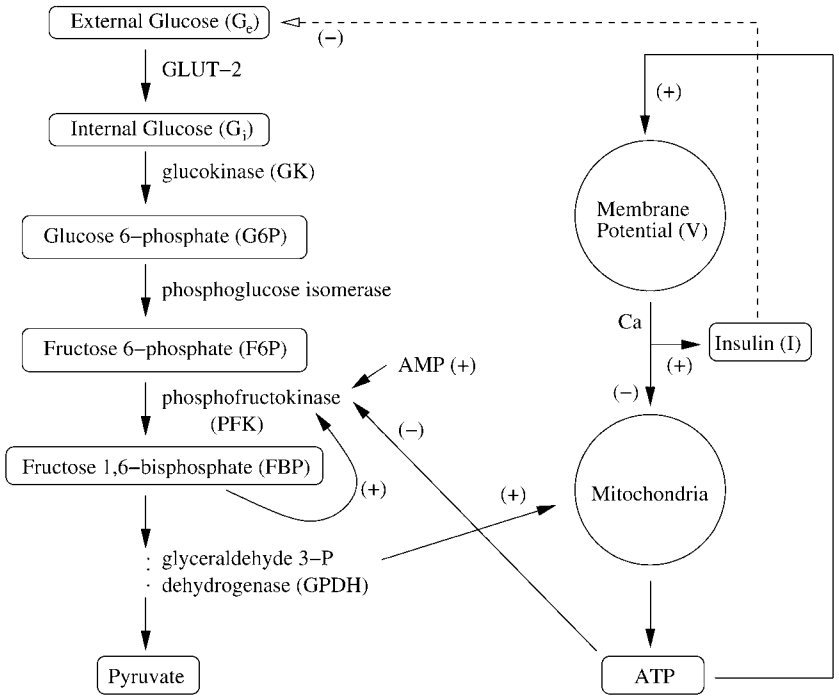

FIGURE 1 An overview of the pathways in the model. Glucose enters the β-cell through GLUT-2 transporters, and is broken down during glycolysis. (*Left column*) Part of the glycolytic pathway, highlighting the enzyme PFK and its regulators. The products of glycolysis feed into the mitochondria where ATP is produced. ATP links the glycolytic component to the electrical component (*right column*) by regulating K(ATP)-channels. These, in turn, regulate membrane potential and Ca^{2+} flow leading to insulin secretion. The electrical/Ca^{2+} component is linked back to glycolysis through Ca^{2+} regulation of ATP production and AMP/ATP feedback onto PFK. (*Dashed line*) Function of insulin to lower the plasma glucose concentration through the actions of the liver. The negative insulin feedback is added to the model when in vivo synchronization is discussed.

is the glyceraldehyde 3-P dehydrogenase (GPDH) reaction rate. The PFK reaction rate, J_{PFK}, reflects the binding of activators (AMP and FBP), an inhibitor (ATP), and the substrate F6P (= 0.3 G6P). ATP is both a substrate and an inhibitor of PFK. As substrate, it is assumed to be saturating, so it is not explicitly included in the model. The PFK reaction rate function is given by

$$J_{\mathrm{PFK}} = V_{\max}\frac{(1-\lambda)w_{1110} + \lambda\sum_{\mathrm{ijl}} w_{\mathrm{ij1l}}}{\sum_{\mathrm{ijkl}} w_{\mathrm{ijkl}}}, \tag{7}$$

where i, j, k, l take value 0 or 1, and

$$w_{\mathrm{ijkl}} = \frac{1}{f_{13}^{\mathrm{ik}} f_{23}^{\mathrm{jk}} f_{41}^{\mathrm{il}} f_{42}^{\mathrm{jl}} f_{43}^{\mathrm{kl}}}\left(\frac{AMP}{K_1}\right)^{\mathrm{i}}\left(\frac{FBP}{K_2}\right)^{\mathrm{j}}\left(\frac{F6P^2}{K_3}\right)^{\mathrm{k}}\left(\frac{ATP^2}{K_4}\right)^{\mathrm{l}}. \tag{8}$$

We refer to Smolen (37) for a discussion of these expressions.

We assume that the total concentration of adenine nucleotides is conserved, and that the adenylate kinase reaction, which converts two molecules of ADP to one molecule of AMP and one of ATP, is at equilibrium $AMP + ADP + ATP = A_{\mathrm{tot}}$, $AMP \times ATP = ADP^2$.

Glycolysis provides input to the mitochondria. Magnus and Keizer (41) developed a model for the mitochondrial production of ATP, in which the production rate decreases with the concentration of free cytosolic Ca^{2+}. In Bertram et al. (6) the Keizer-Magnus model was modified by including the time dynamics of glycolysis. The GPDH reaction rate, J_{GPDH}, is used as a measure of the time-varying input to the mitochondria.

The differential equation for the ADP concentration includes the effects of cytosolic Ca^{2+} concentration (Ca), and the effects of glycolysis:

$$\frac{d\,ADP}{dt} = \frac{1}{\tau_{\mathrm{a}}}\left[ATP - ADP\exp\left((r+\gamma)\left(1-\frac{Ca}{r_1}\right)\right)\right]. \tag{9}$$

The Ca^{2+} effect is through the factor $(1 - (\mathrm{Ca}/\mathrm{r_1}))$; increases in Ca^{2+} concentration lead to increases in ADP. The total substrate-dependent rate is $r + \gamma$. Input from glycolysis is incorporated through the function γ, which depends on the GPDH rate. We describe this with a sigmoidal function of Michaelis-Menten form,

$$\gamma = \frac{\nu_\gamma J_{\mathrm{GPDH}}}{k_\gamma + J_{\mathrm{GPDH}}}, \tag{10}$$

where ν_γ and k_γ are constants. The dependence of ADP on γ (and thus on FBP) is the means through which glycolytic oscillations are transduced into oscillations in nucleotide production. In the earlier Keizer-Magnus model the factor γ was not included (42). The parameter $\tau_{\mathrm{a}} = 5$ min is a slow time constant.

The electrical and Ca^{2+} handling components of the model are based on an earlier β-cell model in which bursting is driven by calcium-dependent oscillations in the K(Ca) current and the K(ATP) current (36). The K(Ca) current is directly activated by calcium. The K(ATP) current conductance is dependent on the concentrations of ADP and ATP; the conductance is lower for higher values of the ratio ATP/ADP. Changes in the cytosolic Ca^{2+} concentration (Ca) take place on a moderately slow timescale (a few seconds to tens of seconds), whereas changes in ADP and ATP occur on a slower timescale (tens of seconds to minutes). The interaction of these two slow processes with disparate timescales can give rise to bursting with periods ranging from a few seconds to a few minutes. This is an example of a phantom bursting model (36,43). The equation for the membrane potential (v) is

$$c_{\mathrm{m}}\frac{d\,v}{dt} = -(I_{\mathrm{K}} + I_{\mathrm{Ca}} + I_{\mathrm{K(Ca)}} + I_{\mathrm{K(ATP)}}), \tag{11}$$

where c_{m} is the membrane capacitance, I_{K} is a v-dependent K^+ current, I_{Ca} is a v-dependent Ca^{2+} current, $I_{\mathrm{K(Ca)}}$ is a calcium-activated K^+ current, and $I_{\mathrm{K(ATP)}}$ is an ATP-sensitive K^+ current, $I_{\mathrm{K}} = \bar{g}_{\mathrm{K}} n(v - v_{\mathrm{K}})$, $I_{\mathrm{Ca}} = \bar{g}_{\mathrm{Ca}} m_\infty(v)(v - v_{\mathrm{Ca}})$, $I_{\mathrm{K(Ca)}} = g_{\mathrm{K(Ca)}}(v - v_{\mathrm{K}})$, and $I_{\mathrm{K(ATP)}} = g_{\mathrm{K(ATP)}}(v - v_{\mathrm{K}})$, where $g_{\mathrm{K(Ca)}} = \bar{g}_{\mathrm{K(Ca)}}(Ca^2/K_{\mathrm{D}}^2 + Ca^2)$, $g_{\mathrm{K(ATP)}} = \bar{g}_{\mathrm{K(ATP)}} o_\infty(ADP, ATP)$.

The equation for the I_{K} activation variable is

$$\frac{d\,n}{dt} = \frac{n_\infty(v) - n}{\tau_{\mathrm{n}}(v)}, \tag{12}$$

where $\tau_n(v) = (1/0.035 \cdot \cosh((v+16)/22.4))$ is the timescale and $n_\infty(v)$ is the equilibrium value of n, $n_\infty(v) = (1/1+\exp(-(v+16)/5.6))$. Activation of Ca^{2+} current is assumed to be instantaneous, with equilibrium function $m_\infty(v) = (1/1+\exp(-(v+20)/12))$.

The K(ATP) conductance is assumed to adjust instantaneously to the concentrations of ADP and ATP, and the form of the conductance function (o_∞) is described in detail in Magnus and Keizer (41). We use the Magnus-Keizer expression for o_∞ without modification:

$$o_\infty(ADP,ATP) = \frac{0.08\left(1+\frac{2\mathrm{MgADP}^-}{17\mu\mathrm{M}}\right)+0.89\left(\frac{\mathrm{MgADP}^-}{17\mu\mathrm{M}}\right)^2}{\left(1+\frac{\mathrm{MgADP}^-}{17\mu\mathrm{M}}\right)^2\left(1+\frac{\mathrm{ADP}^{3-}}{26\mu\mathrm{M}}+\frac{\mathrm{ATP}^{4-}}{1\mu\mathrm{M}}\right)}. \quad (13)$$

As discussed in Magnus and Keizer (41), the nucleotide concentrations are related to the total concentrations of ADP and ATP by $MgADP^{2-} = 0.165\ ADP$, $ADP^{3-} = 0.135\ ADP$, and $ATP^{4-} = 0.005\ ATP$.

The equation for the free cytosolic Ca^{2+} concentration is

$$\frac{d\,Ca}{dt} = f_{\mathrm{cyt}}(J_{\mathrm{mem}} + J_{\mathrm{er}}), \quad (14)$$

where f_{cyt} is the fraction of free to total cytosolic Ca^{2+}, J_{mem} is the Ca^{2+} flux across the plasma membrane, and J_{er} is the Ca^{2+} flux out of the endoplasmic reticulum (ER). The plasma membrane flux term is given by $J_{\mathrm{mem}} = -(\alpha I_{\mathrm{Ca}} + k_{\mathrm{PMCA}}Ca)$, where α converts current to flux, and k_{PMCA} is the Ca^{2+} pump rate. We do not consider the actions of IP3-generating muscarinic agonists, so flux out of the ER is due only to leakage (J_{leak}). Ca^{2+} flux into the ER is through SERCA pumps (J_{SERCA}): $J_{\mathrm{er}} = J_{\mathrm{leak}} - J_{\mathrm{SERCA}}$, where $J_{\mathrm{leak}} = p_{\mathrm{leak}}(Ca_{\mathrm{er}} - Ca)$, $J_{\mathrm{SERCA}} = k_{\mathrm{SERCA}}Ca$, and p_{leak} is the leakage permeability and k_{SERCA} is the SERCA pump rate. The differential equation for the Ca^{2+} concentration in the ER is

$$\frac{d\,Ca_{\mathrm{er}}}{dt} = -f_{\mathrm{er}}(V_{\mathrm{cyt}}/V_{\mathrm{er}})J_{\mathrm{er}}, \quad (15)$$

where f_{er} is analogous to f_{cyt}, and V_{cyt}, V_{er} are the volumes of the cytosolic and ER compartments, respectively.

Finally, we add an equation for insulin secretion to the model from Bertram et al. (6). We describe the rate of insulin secretion, I, by a first-order relation

$$\frac{d\,I}{dt} = \frac{I_\infty(Ca) - I}{\tau_{\mathrm{I}}}, \quad (16)$$

where τ_{I} is a time constant. $I_\infty(Ca)$ is the equilibrium secretion rate, modeled as a linear function of Ca^{2+} (44) by

$$I_\infty(Ca) = \begin{cases} I_{\mathrm{slope}}(Ca - Ca_{\mathrm{null}}) & \text{for} \quad Ca \geq Ca_{\mathrm{null}} \\ 0 & \text{for} \quad Ca < Ca_{\mathrm{null}} \end{cases},$$

where Ca_{null} is the minimal Ca^{2+} concentration necessary for insulin release, and I_{slope} measures the Ca^{2+} sensitivity of secretion. The simple Eq. 16 is motivated by the fact that the most important trigger of insulin release is cytosolic calcium (44–46). For simplicity we do not include the amplifying (K(ATP)-independent) pathway, nor vesicle transportation between different pools. I is measured in arbitrary units.

Values of all parameters used in the model are given in Table 1. Details of the model not described here and discussion of parameters can be found in Bertram et al. (6), Bertram and Sherman (36), Smolen (37), and Magnus and Keizer (41). The differential equations were integrated numerically with the CVODE solver in the software package XPPAUT (47). The computer code for the model can be downloaded from http://www.math.fsu.edu/~bertram or http://mrb.niddk.nih.gov/sherman.

RESULTS

Single-cell simulations

As discussed in Bertram et al. (6), the model can give rise to pulsatile insulin secretion through compound bursting (Fig. 2) with a natural period of ~5 min. The slowest component of the compound bursting is due to oscillatory glycolysis, reflected by an oscillatory FBP concentration (Fig. 2 *A*). This causes slow oscillations in ADP, which superimpose with the faster ADP oscillations driven by Ca^{2+} (Fig. 2 *B*). This multimodal ADP rhythm leads to oscillations in the conductance $g_{\mathrm{K(ATP)}}$ of the ATP-dependent potassium channel, which drives the burst episodes of the membrane potential, v (Fig. 2 *C*). This then gives compound bursting of intracellular calcium (Fig. 2 *D*), leading to pulsatile insulin secretion (Fig. 2 *E*). We show the one-minute moving average of the insulin secretion (Fig. 2 *F*) to facilitate comparison with insulin measurements such as in Sturis et al. (2), where insulin is sampled only about once per minute.

We will be varying the glucose sensitivity parameter V_{gk}. Glycolysis oscillates for intermediate values of this parameter. For V_{gk} too small or too large the glycolytic subsystem is stationary (6). The oscillation period for a range of V_{gk} values is shown in Fig. 3. We note that the period is relatively insensitive to changes in the value of V_{gk}. Importantly, the period is always on the order of several minutes, consistent with data on pulsatile insulin secretion.

Fig. 3 is constructed by finding the period for some V_{gk}, and then we use the endpoint of the previous solution as initial condition for a new solution with V_{gk} slightly changed.

TABLE 1 Parameter values used in the model, except where noted

$V_{\mathrm{glut}} = 8$ mM/ms	$K_{\mathrm{glut}} = 7$ mM	$V_{\mathrm{gk}} = 0.8$ mM/ms	$K_{\mathrm{gk}} = 7$ mM
$n_{\mathrm{gk}} = 4$	$V_{\mathrm{max}} = 2\ \mu$M/ms	$\lambda = 0.06$	$K_1 = 30\ \mu$M
$K_2 = 1\ \mu$M	$K_3 = 50{,}000\ \mu$M	$K_4 = 1000\ \mu$M	$f_{13} = 0.02$
$f_{23} = 0.2$	$f_{41} = 20$	$f_{42} = 20$	$f_{43} = 20$
$A_{\mathrm{tot}} = 3000\ \mu$M	$\nu_\gamma = 2.2$	$k_\gamma = 0.1\ \mu$M/ms	$\tau_a = 300{,}000$ ms
$r = 0.5$	$r_1 = 0.35\ \mu$M	$\bar{g}_{\mathrm{K}} = 2700$ pS	$v_{\mathrm{K}} = -75$ mV
$\bar{g}_{\mathrm{Ca}} = 1000$ pS	$v_{\mathrm{Ca}} = 25$ mV	$\bar{g}_{\mathrm{K(Ca)}} = 400$ pS	$K_{\mathrm{D}} = 0.5\ \mu$M
$\bar{g}_{\mathrm{K(ATP)}} = 40{,}000$ pS	$c_{\mathrm{m}} = 5300$ fF	$V_{\mathrm{cyt}}/V_{\mathrm{er}} = 31$	$p_{\mathrm{leak}} = 0.0002\ \mathrm{ms}^{-1}$
$f_{\mathrm{cyt}} = 0.01$	$f_{\mathrm{er}} = 0.01$	$k_{\mathrm{PMCA}} = 0.18\ \mathrm{ms}^{-1}$	$k_{\mathrm{SERCA}} = 0.4\ \mathrm{ms}^{-1}$
$\tau_{\mathrm{I}} = 10{,}000$ ms	$I_{\mathrm{slope}} = 210\ \mu\mathrm{M}^{-1}$	$Ca_{\mathrm{null}} = 0.055\ \mu$M	$\kappa = 0.005$
$\alpha = 4.5 \cdot 10^{-6}\ \mu$M/ms			

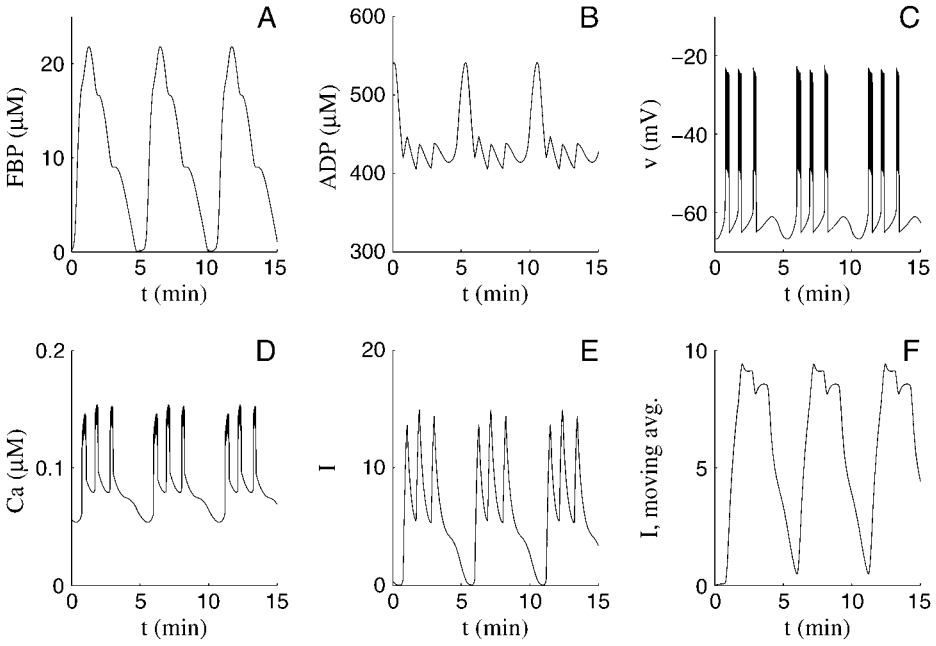

FIGURE 2 Compound bursting leading to pulsatile insulin secretion for a constant glucose stimulus, $G_e = 7$ mM, with $V_{gk} = 0.8$ mM/ms. The period of the pulses is 5.2 min.

When increasing V_{gk} (Fig. 3, *solid curve*) the system follows a branch of stable periodic solutions, corresponding to pulsatile insulin secretion, until such a periodic solution no longer exists at $V_{gk} = 0.84$ mM/ms. The system then follows the branch of steady states, corresponding to constant insulin release with small oscillations that reflect simple bursting. For decreasing V_{gk} (Fig. 3, *dashed curve*) the system follows this branch of steady states until the steady state loses its stability at $V_{gk} = 0.74$ mM/ms. The system then follows the branch of periodic solutions for lower V_{gk} values.

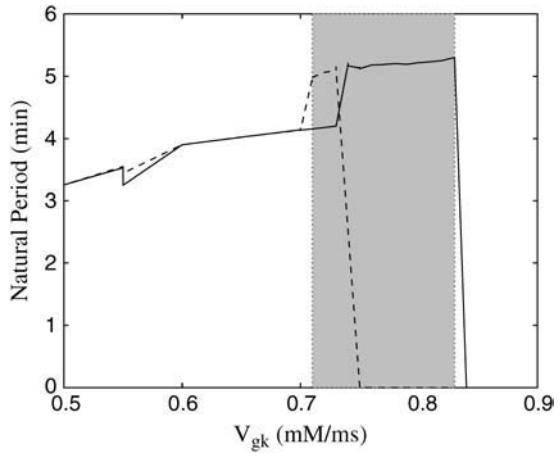

FIGURE 3 The natural period of the pulsatile insulin secretion as a function of the glucose sensitivity parameter V_{gk}. The solid curve is produced by increasing V_{gk}, using the previous solution as initial conditions, whereas the dashed line is generated by decreasing V_{gk}. The shaded area indicates the region of bistability between stationary glycolysis and oscillatory glycolysis.

Note that there is bistability for V_{gk} between 0.71 and 0.83 mM/ms. Thus, pulsatile insulin release patterns and constant release patterns coexist, corresponding to a coexisting periodic solution and a stable stationary state of the glycolytic subsystem. The values of the initial conditions determine which behavior is produced. This model prediction was confirmed experimentally in Bertram et al. (6). We also note that another type of bistability, consisting of two coexisting periodic solutions, is present for V_{gk} near 0.71 mM/ms. We hypothesize that this corresponds to an S-shaped periodic branch where the two stable branches shown in Fig. 3 with periods ~4 and 5 min, respectively, are connected with a branch of unstable periodic solutions, which is created and destroyed in two saddle-node bifurcations.

Intra-islet synchronization

It is well established that electrical and Ca^{2+} oscillations of β-cells are synchronized within an islet (10,48–51), a necessary fact in order to see a pulsatile insulin signal from an islet. This synchronization is impaired in islets from ob/ob mice (10). If glycolysis is driving pulsatile secretion, then metabolism should be synchronized throughout the islet. This metabolic synchronization was demonstrated by Jung et al. (52), who showed that oxygen levels measured at two different sites in an islet were synchronized.

Although it is generally believed that gap junctions synchronize cells via electrical coupling, it is also possible that gap junctions are permeable to glycolytic intermediaries. By allowing FBP to diffuse between two cells, we can easily obtain synchronization of both insulin secretion and glycolysis. This is possible even for very low diffusion rates and without electrical coupling (simulations not shown). On the

other hand, electrical oscillations can be synchronized by electrical coupling through gap junctions (53).

More surprisingly, we now show that electrical coupling alone can synchronize glycolytic oscillations without the need for the diffusion of glycolytic intermediates. We model the electrical coupling between two cells by adding

$$-g_c(v_i - v_j) \tag{17}$$

to Eq. 11 for cell $i = 1, 2, j \neq i$.

In this case v and c are synchronized by the electrical coupling (not shown), leading to synchronized secretion (Fig. 4 *A*). Surprisingly, glycolytic oscillations also synchronize when the two cells are electrically coupled (Fig. 4 *B*). The figure also illustrates that the average insulin secretion signal is not clearly pulsatile when the cells are uncoupled, since the two glycolytic oscillations are often out of phase. This lack of phasing would be more pronounced with more cells.

The mechanism behind the synchronization is that the coupling rapidly synchronizes electrical activity. This then synchronizes Ca^{2+} levels and, consequently, insulin release (Fig. 4 *A*). Synchronization of metabolism takes longer to achieve (Fig. 4 *B*), due to the indirect manner in which Ca^{2+} affects the glycolytic oscillator. The Ca^{2+} inhibits mitochondrial ATP production, thus disinhibiting PFK activity. Without Ca^{2+} feedback onto ATP production, or ATP and AMP feedback onto PFK, synchronization of glycolysis would not occur, even though gap junctions could synchronize electrical activity. This is illustrated for the case of no Ca^{2+} feedback in Fig. 5, where the glycolytic oscillator drives pulsatile insulin release. The electrical subsystem synchronizes when the cells are coupled leading to synchronized insulin secretion (Fig. 5 *A*) but the glycolytic subsystems do not synchronize (Fig. 5 *B*).

Interestingly, in Fig. 4 there is virtually no insulin secretion at $\sim t = 20$ min, even though the average FBP concentration is fairly high. The FBP concentrations of the two cells are out of phase, and one is low at $t = 20$ min. So, if uncoupled at any time at $\sim t = 20$ min, one of the cells would be silent and the other one would be active. Fig. 4 shows that the silent cell is enough to terminate the (synchronized) insulin secretion. The same phenomenon is seen in Fig. 5. This points to the importance of having synchronized glycolysis, since insulin release is lower when glycolysis is out of phase.

The period of the coupled cells is similar to that of the faster of the two uncoupled cells. Thus, the faster cell drives the slow cell when coupled.

Entrainment by a rhythmic glucose stimulus

Several labs have examined the entrainability of insulin secretion from the perfused pancreas, groups of islets, and single islets (1,2). They found that in all three cases it is possible to entrain the insulin secretion to an oscillating glucose stimulus. Moreover, slow NAD(P)H, Ca^{2+}, and mitochondrial membrane potential oscillations, which are thought to underlie pulsatile insulin release, can be entrained in mouse islets (32). Finally, it has been confirmed in vivo that pulsatile insulin release can be entrained to a periodic glucose infusion (29,30). We next demonstrate that it is possible to entrain our model cells with a low-amplitude glucose stimulus, and that the period of the entrained oscillation can be lower or greater than the natural period.

Sturis et al. (2) showed that pulsatile insulin secretion from an isolated pancreas and from isolated islets can be entrained by a sinusoidal glucose stimulus with amplitude as low as 5% of the mean. The present model describes the behavior of a representative cell located in an islet, and indeed, applying a sinusoidal external glucose stimulus to the model entrains the insulin secretion (Fig. 6). In Fig. 6 *A*, the natural pulsatility for $V_{gk} = 0.8$ mM/ms with a period of ~5 min is

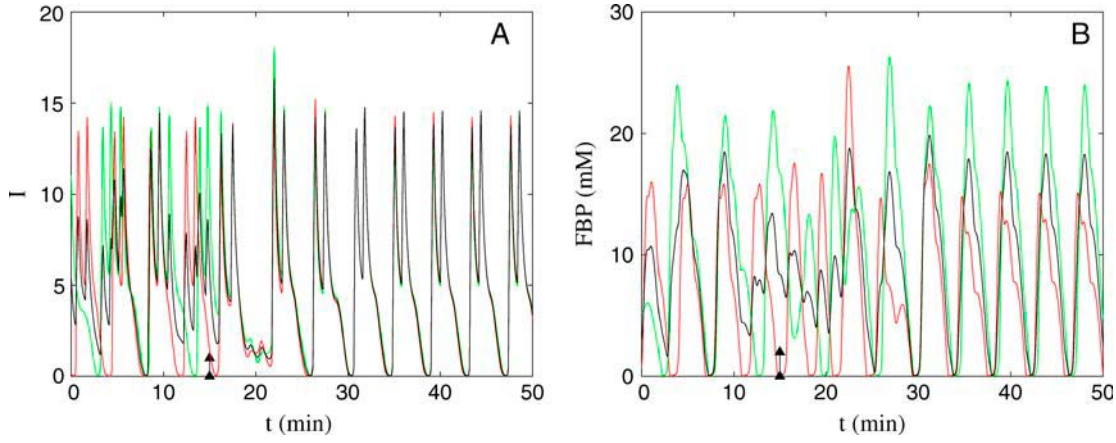

FIGURE 4 Two cells become synchronized when electrically coupled. Parameters as in Fig. 2, except $V_{gk,\,1} = 0.6$ mM/ms, $V_{gk,\,2} = 0.8$ mM/ms, and g_c is raised from 0 pS to 100 pS at $t = 15$ min (*arrow*). (*A*) Rapid synchronization of insulin secretion. Red is the faster I_1, green is the slower I_2, and black is the average insulin secretion $\bar{I}$ from the two cells. (*B*) Slower synchronization of glycolysis. Red is FBP_1, green is FBP_2, and black is the average of the two cells.

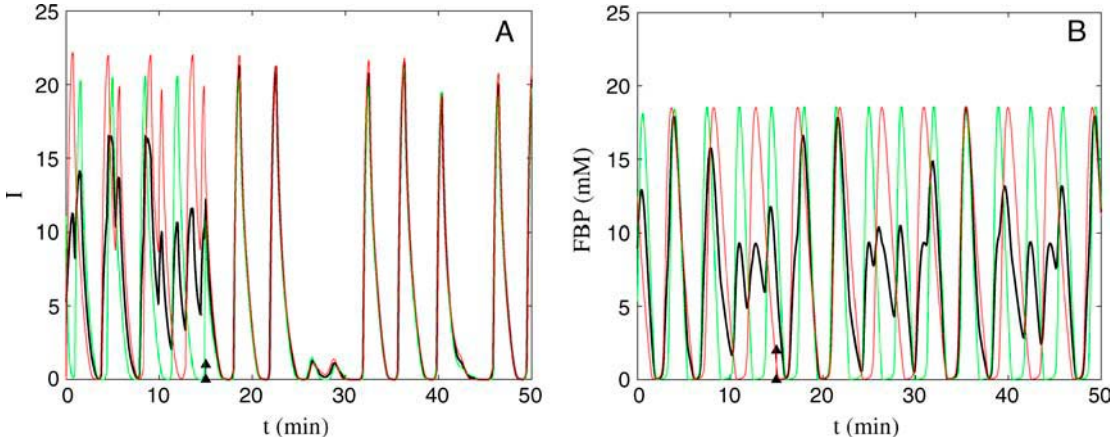

FIGURE 5 Without Ca^{2+} feedback the cells do not synchronize glycolysis when electrically coupled. The absence of feedback is attained by keeping $Ca = 0.1\ \mu$M constant in Eq. 9. The parameters are as in Table 1 except $V_{gk,\,1} = 0.6$ mM/ms, $V_{gk,\,2} = 0.5$ mM/ms, $\kappa_1 = 0.003$, $\kappa_2 = 0.004$, $\bar{g}_{K,\,ATP} = 37{,}000$ pS, and g_c is raised from 0 pS to 100 pS at $t = 15$ min (*arrow*). (*A*) Rapid synchronization of insulin secretion. Red is the slower I_1, green is the faster I_2, and black is the average insulin secretion $\bar{I}$ from the two cells. (*B*) Lack of synchronization of glycolysis. Red is FBP_1, green is FBP_2, and black is the average of the two cells.

shown. This pulsatile secretion is entrained to a faster (4-min period, Fig. 6 *B*) as well as to a slower (7-min period, Fig. 6 *C*) periodic glucose stimulus. However, for $V_{gk} = 0.6$ mM/ms the entrainment is impaired; the pulses are no longer entrainable to a glucose signal with period of 7 min (Fig. 6 *D*). In all cases, the external glucose concentration oscillates at ~7 mM on average, with 1-mM amplitude. The insulin pulses are in phase with the maximal glucose concentrations when forced by slower glucose oscillations as found by Sturis et al. (2).

As demonstrated in Fig. 6, it is possible to entrain the model β-cells at periods shorter or longer than the natural period. The entrainment window depends on the amplitude of the glucose oscillations and on the glucose sensitivity parameter V_{gk}. Fig. 7 shows the entrainment windows for a range of values of V_{gk}, with the glucose oscillation amplitude fixed at 1 mM. Note that the range of entrainment periods is larger when we enter the region with bistability ($V_{gk} > 0.7$ mM/ms, see Fig. 3) and larger yet in the region with no unforced glycolytic oscillations. In this region, the forced system has a clearly pulsatile behavior even though the unforced system does not. This is because the varying glucose concentration, which is similar to varying V_{gk}, pushes the system into the region with oscillatory glycolysis.

Electrical coupling between cells within an islet facilitates the entrainment of the heterogeneous cell population of the islet. Cell number one (*red*) in Fig. 4 with $V_{gk} = 0.6$ mM/ms is difficult to entrain, i.e., the cell is only entrainable in a narrow interval of forcing periods, see Fig. 6 *D* and Fig. 7. However, when coupled to cell number two (*green*), which is easier to entrain ($V_{gk} = 0.8$ mM/ms), the cell pair is entrainable (Fig. 8), even though one of the two cells was not entrainable when uncoupled. In this way, the coupling between cells not only synchronizes the secretion within the islet but also helps the islet to synchronize to an external glucose signal. If the cells were uncoupled, some would not follow the external signal because of heterogeneity of cell properties, and the overall response from the collection of cells (the islet) would not follow the glucose stimulus as nicely as shown in Fig. 8.

We can regard the pancreas as an assembly of many uncoupled islets, and the mechanism for the entrainment of the pancreas could be the following. With a constant glucose concentration the islets drift with respect to each other, so that even though each islet gives a pulsatile insulin signal, the total signal will be relatively flat; it has been averaged over all the islets. But when the glucose concentration oscillates, the islets synchronize their insulin secretion so that the total signal will be clearly pulsatile.

To illustrate this, we simulate 20 uncoupled islets with different glucose sensitivity (V_{gk} chosen from a uniform distribution between 0.6 and 0.9 mM/ms) with glucose concentration first constant, then oscillatory, and then constant again. (Here and in the following we represent each islet as a single cell whose properties are the average of those in the islet.) Fig. 9 shows that the islets start off desynchronized and the average signal consists of small irregular pulses. When the glucose stimulus oscillates, the islets synchronize and the average signal becomes clearly pulsatile.

In vivo inter-islet synchronization

Several in vivo studies have shown that in healthy humans, pulsatile insulin secretion can be entrained to rhythmic glucose stimuli with periods of 7–12 min (30) or, yielding a more complex pattern, to pulses every 29 min (29), demonstrating that the pancreas is tightly controlled by the fast oscillations in plasma glucose levels that occur in vivo (26–30). Although ultradian oscillations are also entrained to

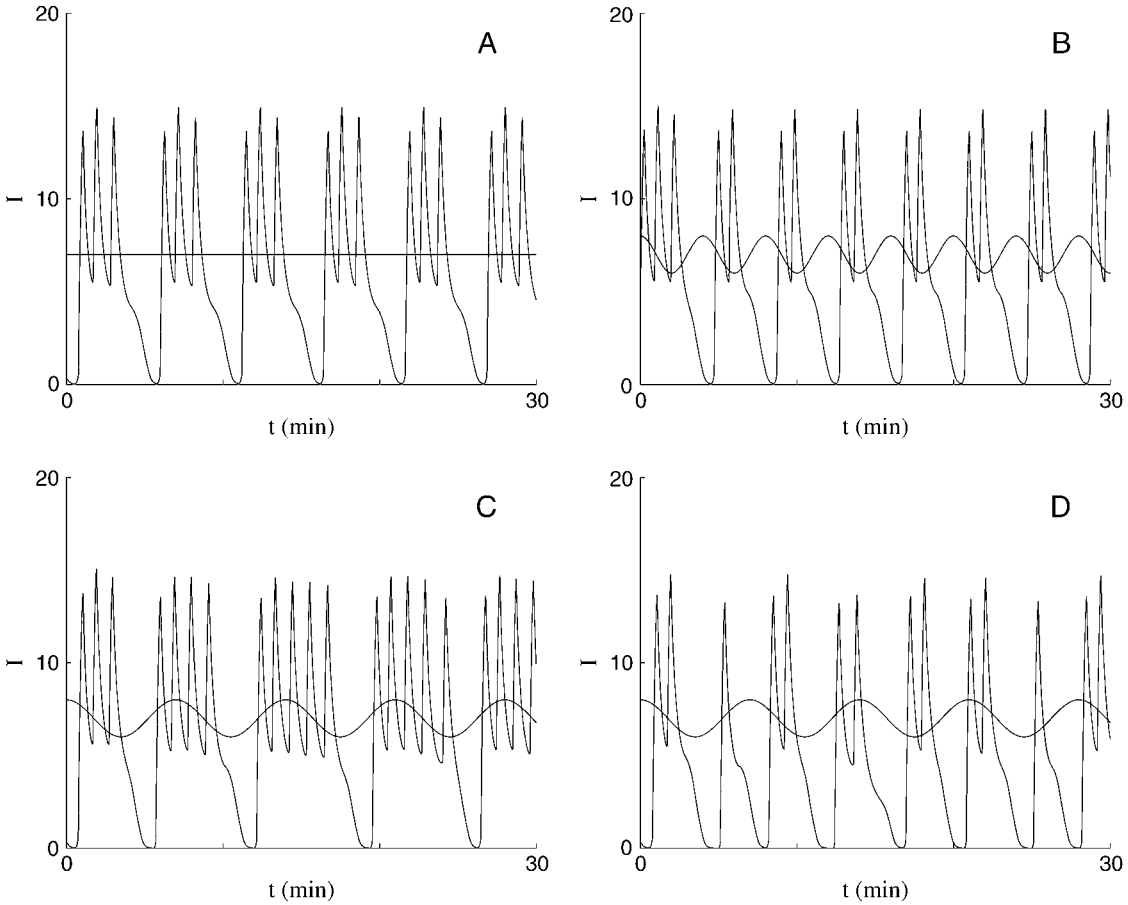

FIGURE 6 Entrainment of the pulsatile insulin secretion to a sinusoidal glucose stimulus. (*A*) The natural pulsatile insulin secretion with $V_{gk} = 0.8$ mM/ms and constant $G_e = 7$ mM. The period of the pulses is ~5 min. (*B*) Entrainment to a faster oscillating glucose stimulus with a period of 4 min. $V_{gk} = 0.8$ mM/ms. (*C*) Entrainment to a slower oscillating glucose stimulus with a period of 7 min. $V_{gk} = 0.8$ mM/ms. (*D*) Lack of entrainment to a glucose stimulus with a period of 7 min when V_{gk} is reduced to 0.6 mM/ms. All glucose oscillations are centered at $\sim G_e = 7$ mM with 1 mM amplitude.

periodic infusions (31), the underlying mechanisms seem to be different. Ultradian oscillations are believed to be created by glucose/insulin feedback (31,54), and the infusions interact directly with this feedback system. For the faster insulin pulses under investigation here, the glucose stimulus rather seems to have a synchronizing role of the oscillating secretion from individual cells and islets.

We have shown that oscillations in the extracellular glucose concentration can synchronize insulin secretion. In vivo, hepatic glucose production follows plasma insulin oscillations (27), which suggests a mechanism by which pulsatile insulin release leads to periodic glucose production and plasma glucose levels. We investigate next whether insulin itself, through its action on the liver, could produce oscillations in the glucose concentration that could then entrain insulin secretion from the islets, as proposed by several authors (2,3,20,21).

To our model system we add a very simple representation of the liver, modeled by a first order equation for the dynamic response of plasma glucose, G_e, to the average insulin secretion $\bar{I}$,

$$\frac{dG_e}{dt} = \frac{G_\infty(\bar{I}) - G_e}{\tau_G}, \tag{18}$$

where G_∞ is a decreasing sigmoidal function,

$$G_\infty(\bar{I}) = G_{min} + \frac{G_{max} - G_{min}}{1 + \exp\left(\dfrac{\mathrm{I} - \hat{\mathrm{I}}}{\mathrm{S_G}}\right)}. \tag{19}$$

Here G_{min} corresponds to a very high insulin concentration, whereas G_{max} corresponds to a very low insulin concentration. The value $\hat{I}$ is the insulin secretion, which gives the half-maximal glucose level, $G_e = (1/2)(G_{max} + G_{min})$. The parameters are listed in Table 2. Note that the timescale set by $\tau_G = 7.5$ min allows the liver to respond to changes in insulin release on a scale of minutes. This is in contrast to the much slower response time used in the models of ultradian oscillations (34,54).

In Fig. 10 *A* we see that we can synchronize 20 islets using this model for the external glucose feedback, even though the islets are not directly (e.g., electrically) coupled to each

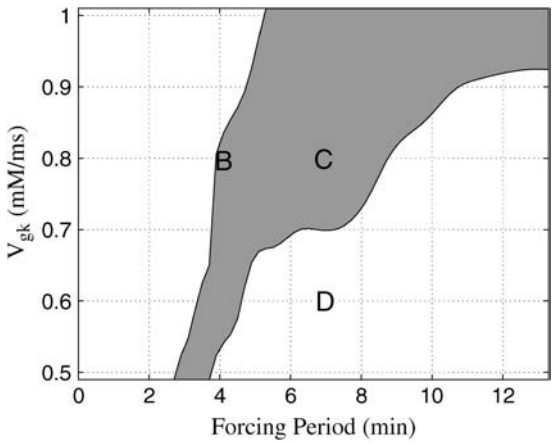

FIGURE 7 The entrainment window (*shaded*) for a range of values of V_{gk} and period of the G_e oscillations (*Forcing Period*). Glucose oscillations are 1 mM in amplitude, with an approximate mean value of 7 mM. *B–D* correspond to the panels in Fig. 6.

other. We begin by keeping G_e constant, and then at time $t = 20$ min we let G_e vary according to Eq. 18. Soon afterwards the previously unsynchronized islets become synchronized, resulting in a clearly pulsatile insulin signal, even though the individual bursts are out of phase as found in vivo (51); only the burst episodes are in phase. This is reflected in the lack of large-amplitude spikes on top of the slow pulses in the average insulin release (Fig. 10 *A*), in contrast to the intra-islet synchronization (Fig. 4 *A*).

Synchronization by feedback from the liver is possible even for islets that would not give pulsatile secretion in constant glucose, but when the glucose begins to oscillate they become entrained, which results in a pulsatile signal. Fig. 10 *B* shows a simulation of nine islets with $V_{gk} \geq 0.87$ mM/ms. Glycolysis does not oscillate in any of these islets when $G_e = 7$ mM is constant. At time $t = 10$ min we let G_e vary as before and now a pulsatile insulin signal emerges. Note that, in constant glucose, the islets release insulin in fast pulses as observed experimentally in vitro (55,56). These fast fluctuations are driven by bursting electrical activity since glycolysis is stable. They are of much smaller amplitude than the slower pulses driven by glycolysis, due to the lack of synchrony of individual bursts between islets. Thus, bursting electrical activity can drive insulin oscillations, but it is not likely to drive the slower insulin pulsatility with a period of several minutes.

The difference between dynamic and constant extracellular glucose is even clearer in Fig. 11 *A*, where the smoothed insulin secretion from Fig. 10 *A* is compared with the secretion with a fixed glucose concentration. The power spectrum of the two curves beyond the point where the glucose concentration is allowed to vary (after a 10-min transient phase) confirms that the insulin secretion is much more pulsatile when G_e is allowed to vary and the islets synchronize (Fig. 11 *B*). However, even in constant glucose the average insulin secretion oscillates. This is due to the fact that the drifting between the islets leads to times when some of the islets are nearly in phase, resulting in pulses of insulin secretion.

These observations could mean that pulsatile insulin secretion would be seen more often and be more regular in vivo than in vitro, where G_e is usually kept constant. This observation is confirmed by the fact that, in vivo, >70–75% of the total insulin secretion is released in bursts (35,57,58), whereas the corresponding fraction in vitro is <40% (23,59). Moreover, the in vitro pulses from the perfused pancreas are less regular than the in vivo pulses when analyzed by autocorrelation (20).

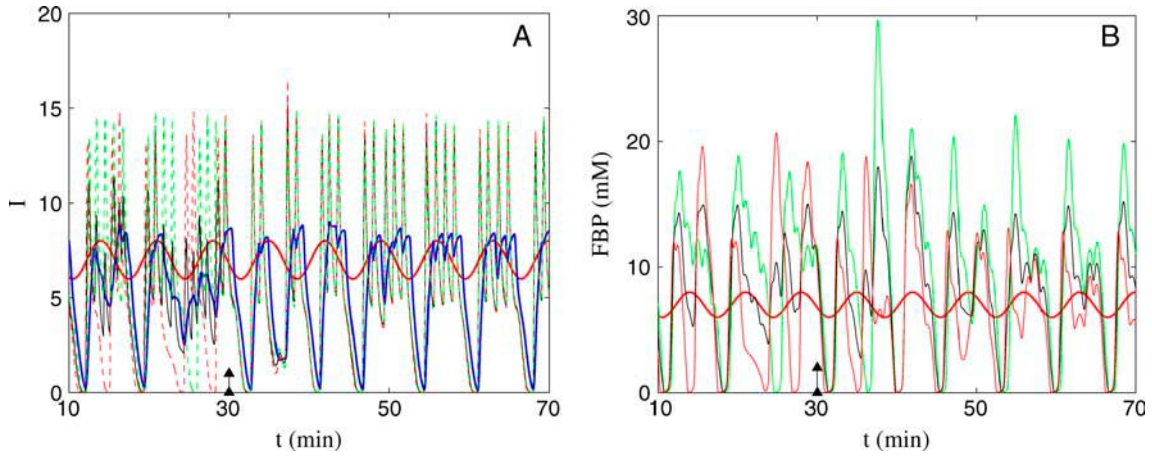

FIGURE 8 Two cells are entrainable to a stimulus with a larger period when coupled. Parameters as in Fig. 4, except g_c is raised from 0 pS to 100 pS at $t = 30$ min (*arrow*). The glucose concentration (*sinusoidal red curves*) oscillates with a period of 7 min and amplitude of 1 mM. (*A*) Entrainment of insulin secretion. Red is the faster non-entrainable cell, green is the slower entrainable cell, and black is the average insulin secretion $\bar{I}$ from the two cells. The blue curve is the 1-min moving average of $\bar{I}$. (*B*) Entrainment of glycolysis. The color scheme is the same as in *A*.

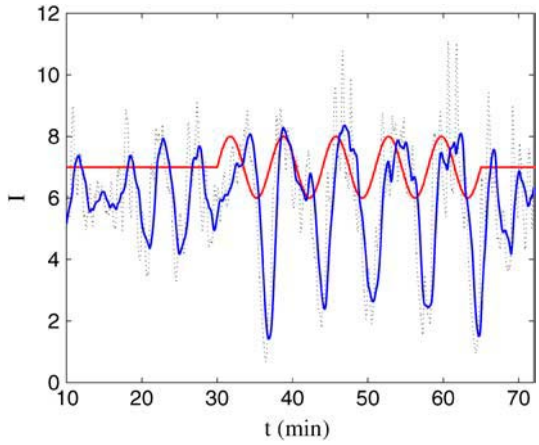

FIGURE 9 A population of 20 islets becomes synchronized by an oscillatory glucose stimulus, resulting in pulsatile insulin secretion. The figure shows the insulin secretion averaged over the 20 islets (*dotted black line*), the average insulin secretion smoothed using a 1-min moving average (*blue*), and the glucose concentration (*red*), which is either constant or oscillatory with a period of 7 min and an amplitude of 1 mM. $V_{gk,\,i}$, $i = 1, \ldots,$ 20 are randomly chosen from a uniform distribution over [0.6, 0.9] mM/ms.

DISCUSSION

The role of the glycolytic oscillator could be to add a component slower than that driving bursting so that β-cells are capable of resonating with a feedback signal (glucose) from the body. The timescale of insulin signaling in the liver is on the order of 5–15 min (12–14,60,61), and the sensitivity of the liver to pulsatile insulin is frequency-dependent (14), which indicates that, for optimal functioning, the β-cells would need a system sensing as well as secreting on the timescale of insulin signaling. The glycolytic pathway is ideal for sensing glucose feedback, since glucose is a substrate for glycolysis. Furthermore, the period of the glycolytic oscillator is relatively insensitive to changes in plasma glucose concentration (Fig. 3). This frequency-insensitivity is consistent with studies that have shown that it is primarily the amplitude of the pulsatile insulin secretion, rather than the period, that is affected by changes in the glucose concentration (3,23,35,58,59).

In this scenario, the glycolytic oscillator produces insulin pulses with a period of 5 min, which is of the ideal timescale for optimal insulin sensitivity in the liver. The liver responds to the insulin pulses so that the plasma glucose concentration oscillates, which then entrains the population of islets, in this way regularizing and amplifying the insulin release pattern (Figs. 10 and 11). For this to work, the entrainability of each islet is crucial. The model presented here can be entrained by both faster and slower glucose oscillations (Fig. 6), and this mechanism indeed synchronizes the insulin pulses from uncoupled islets (Fig. 9).

TABLE 2 Parameter values defining the response of plasma glucose, G_e, to the average insulin secretion $\bar{I}$

$G_{min} = 1$ mM	$G_{max} = 15$ mM	$\tau_G = 450{,}000$ ms	$S_G = 1$	$\hat{I} = 5$

In contrast, it has been suggested that an intrapancreatic, neuronal pacemaker is responsible for synchronizing the pulsatile insulin secretion from the many islets in the pancreas (3,19,25). However, as mentioned, and studied previously (2,24,39), this would not explain how single islets or groups of islets can be entrained. If a pancreatic pacemaker was solely responsible for the entrainment, then this effect would be lost when the islets were separated from the pancreas. Furthermore, in Sha et al. (25) pulsatile insulin secretion was observed from a piece of the pancreas, even though the intrapancreatic ganglion nerves were electrically silent, showing that neuronal activity is not essential for at least some degree of synchrony and pulsatile release. We showed that the entrainability of each cell, and hence each islet, is sufficient to provide the synchronization mechanism (Figs. 10 and 11). However, it cannot be ruled out that a neuronal pacemaker mechanism enhances this effect in vivo. Indeed, pulsatile insulin secretion has been observed in conditions of constant glucose (19,35), arguing for a role of a neuronal pacemaker.

The first step toward a pulsatile signal from the pancreas is the pulsatile secretion from the individual islets. Fig. 4 showed that electrical coupling of the cells through gap junctions is enough to synchronize not only the membrane potential, intracellular calcium, and insulin secretion, but the glycolytic oscillations as well. Two essential elements for synchronization in our model are the feedback of Ca^{2+} onto the mitochondria (Fig. 5) and the feedback of AMP and ATP onto PFK. Without these feedback pathways the membrane potential, which is coupled to the membrane potential of neighboring cells through gap junctions, could not be communicated to the glycolytic subsystem, and it would not be possible for electrical coupling to synchronize glycolytic oscillations. Our simulations showed that if glycolysis is not synchronized, there is less insulin secretion (Figs. 4 and 5). The positive effects of glycolytic synchronization would be accentuated by any K(ATP)-independent glucose pathway (45), since amplifying signals would plausibly be in phase with the glycolytic oscillator. If the calcium levels in different cells were in synchrony, but the glycolytic components were not, then the amplifying signals would not be synchronized, and thus would not have maximal effect. Finally, we do not count out the possibility that synchronization of glycolytic oscillations could be aided by the diffusion through gap junctions of glycolytic intermediates, ATP, or other signaling molecules.

It was demonstrated in Fig. 4 that gap-junctional coupling between cells leads to a pulsatile secretion with a period close to that of the fastest of the cells. Moreover, this coupling enhances the entrainability of the islets to plasma glucose feedback (Fig. 8). This shows an advantage of having the cells clustered into islets and not scattered around in the pancreas as single cells.

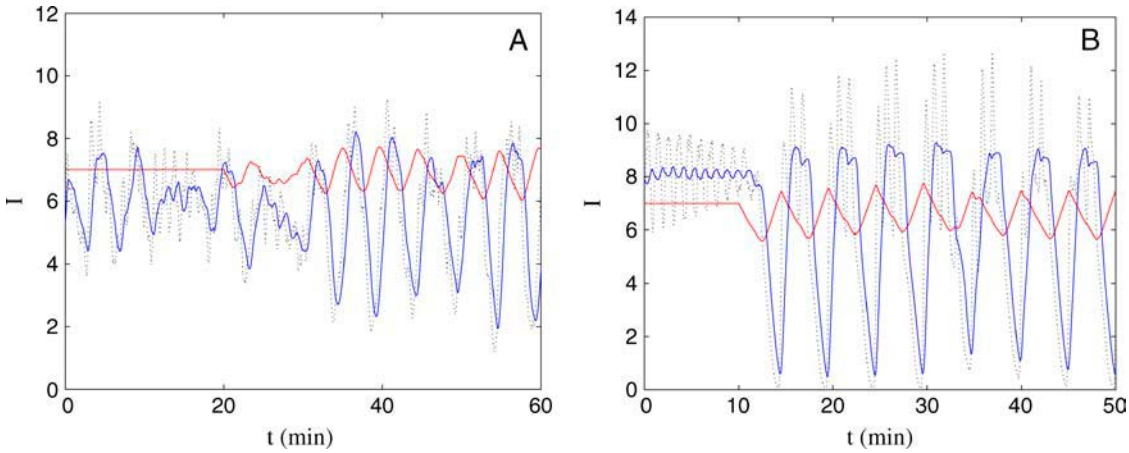

FIGURE 10 (*A*) 20 islets become synchronized when coupled through the plasma glucose concentration. The value G_e is dynamic from $t = 20$ min. Legends and $V_{gk,\,i}$ as in Fig. 9. (*B*) Islets without pulsatile secretion can become pulsatile when coupled through the plasma glucose concentration. The value G_e is dynamic from $t = 10$ min. $V_{gk,\,i} = 0.85 + 0.02i$ mM/ms, $i = 1, \ldots, 9$.

The present model can undergo 2:1 entrainment, meaning that for each period of the glucose oscillations we have two pulses of insulin release (simulations not shown). The 2:1 entrainment is a general phenomenon of forced oscillatory systems and is also observed for ultradian oscillations (34). Such 2:1 entrainment was recently observed for entrainment of NAD(P)H, Ca^{2+}, and mitochondrial membrane potential oscillations (32). It was also observed in an in vivo study with human patients (29). We will continue the investigation of various kinds of entrainment in a future article.

We have previously proposed ''the metronome model'' for insulin secretion (6). The idea is that, whereas the glycolytic component is responsible for setting the period of the insulin pulses (the metronome), the electrical component is responsible for the pulse mass (the amplitude of the beat of the metronome). Although the period of the metronome is relatively insensitive to the glucose level, the amplitude is highly sensitive, and is adjusted by modulating the plateau fraction of bursting in response to changes in the glucose level. The K(ATP)-independent, amplifying pathway could further accentuate the effects of glucose on the pulse amplitude. This model provides a way for the β-cells to meet two demands: matching the frequency to the timescale of the target issues and being able to adjust the insulin secretion level to match the demands of the body. It also gives a *raison d'être* for both the glycolytic oscillator and for the electrical bursting behavior. We have shown here that the metronome model is consistent with the experimental findings that β-cells are synchronized within an islet, that islets can be entrained by sinusoidal glucose oscillations, and that insulin secretion is oscillatory in vivo.

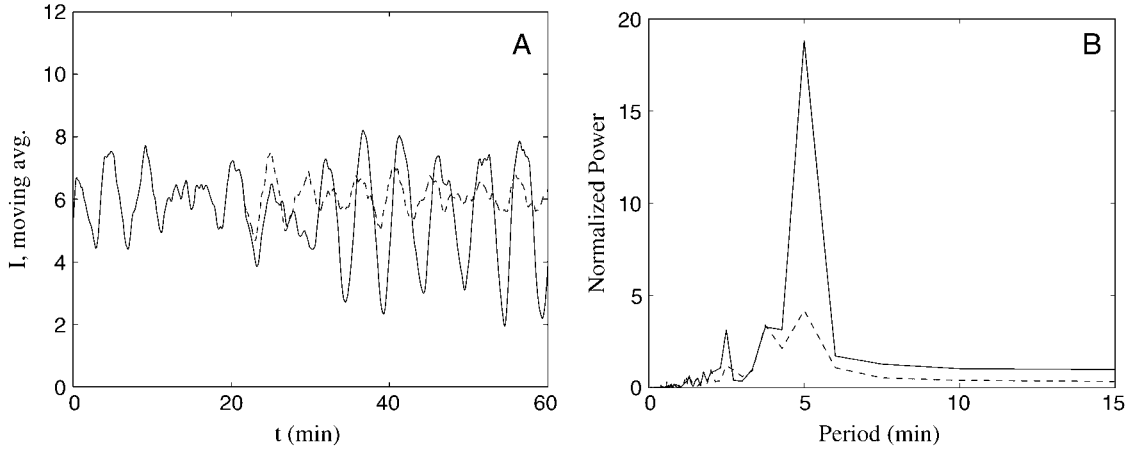

FIGURE 11 (*A*) The smoothed insulin signal from Fig. 10 *A* (*blue curve*) is compared to the smoothed insulin signal when the glucose concentration remains fixed (*black dashed curve*). (*B*) The normalized power spectra of the two signals from the last 30 min (*t* from 30 to 60 min) of *A* with dynamic (*blue curve*) or fixed (*black dashed curve*) glucose concentration.

M.G.P. thanks the Laboratory of Biological Modeling, National Institute of Diabetes and Digestive and Kidney Diseases, National Institutes of Health, for letting him visit the lab, where this work was initiated.

M.G.P. was partially supported by ''Rejselegat for Matematikere'' (Travelling Scholarship for Mathematicians). R.B. was supported by National Science Foundation grant No. DMS-0311856.

REFERENCES

1. Chou, H. F., and E. Ipp. 1990. Pulsatile insulin secretion in isolated Rat islets. *Diabetes.* 39:112–117.
2. Sturis, J., W. L. Pugh, J. Tang, D. M. Ostrega, J. S. Polonsky, and K. S. Polonsky. 1994. Alterations in pulsatile insulin secretion in the Zucker diabetic fatty rat. *Am. J. Physiol. Endocrinol. Metab.* 267:E250–E259.
3. Pørksen, N. 2002. The in vivo regulation of pulsatile insulin secretion. *Diabetologia.* 45:3–20.
4. Longo, E. A., K. Tornheim, J. T. Deeney, B. A. Varnum, D. Tillotson, M. Prentki, and B. E. Corkey. 1991. Oscillations in cytosolic free Ca^{2+}, oxygen consumption, and insulin secretion in glucose-stimulated Rat pancreatic islets. *J. Biol. Chem.* 266:9314–9319.
5. Tornheim, K. 1997. Are metabolic oscillations responsible for normal oscillatory insulin secretion? *Diabetes.* 46:1375–1380.
6. Bertram, R., L. Satin, M. Zhang, P. Smolen, and A. Sherman. 2004. Calcium and glycolysis mediate multiple bursting modes in pancreatic islets. *Biophys. J.* 87:3074–3087.
7. Lang, D. A., D. R. Matthews, M. Burnet, and R. C. Turner. 1981. Brief, irregular oscillations of basal plasma insulin and glucose concentrations in diabetic man. *Diabetes.* 30:435–439.
8. O'Rahilly, S., R. C. Turner, and D. R. Matthews. 1988. Impaired pulsatile secretion of insulin in relatives of patients with non-insulin-dependent diabetes. *N. Engl. J. Med.* 318:1225–1230.
9. Schmitz, O., N. Pørksen, B. Nyholm, C. Skjærbæk, P. C. Butler, J. D. Veldhuis, and S. M. Pincus. 1997. Disorderly and nonstationary insulin secretion in relatives of patients with NIDDM. *Am. J. Physiol. Endocrinol. Metab.* 272:E218–E226.
10. Ravier, M. A., J. Sehlin, and J. C. Henquin. 2002. Disorganization of cytoplasmic Ca^{2+} oscillations and pulsatile insulin secretion in islets from ob/ob mice. *Diabetologia.* 45:1154–1163.
11. Matthews, D. R., B. A. Naylor, R. G. Jones, G. M. Ward, and R. C. Turner. 1983. Pulsatile insulin has greater hypoglycemic effect than continuous delivery. *Diabetes.* 32:617–621.
12. Bratusch-Marrain, P. R., M. Komjati, and W. K. Waldhausl. 1986. Efficacy of pulsatile versus continuous insulin administration on hepatic glucose production and glucose utilization in type I diabetic humans. *Diabetes.* 35:922–926.
13. Komjati, M., P. Bratusch-Marrain, and W. Waldhausl. 1986. Superior efficacy of pulsatile versus continuous hormone exposure on hepatic glucose production in vitro. *Endocrinology.* 118:312–319.
14. Paolisso, G., A. J. Scheen, D. Giugliano, S. Sgambato, A. Albert, M. Varricchio, F. D'Onofrio, and P. J. Lefebvre. 1991. Pulsatile insulin delivery has greater metabolic effects than continuous hormone administration in man: importance of pulse frequency. *J. Clin. Endocrinol. Metab.* 72:607–615.
15. Ashcroft, F. M., and P. Rorsman. 1989. Electrophysiology of the pancreatic β-cell. *Prog. Biophys. Mol. Biol.* 54:87–143.
16. Cook, D. L. 1983. Isolated islets of Langerhans have slow oscillations of electrical activity. *Metabolism.* 32:681–685.
17. Henquin, J. C., H. P. Meissner, and W. Schmeer. 1982. Cyclic variations of glucose-induced electrical activity in pancreatic B cells. *Pflugers Arch.* 393:322–327.
18. Zhang, M., P. Goforth, R. Bertram, A. Sherman, and L. Satin. 2003. The Ca^{2+} dynamics of isolated Mouse β-cells and islets: implications for mathematical models. *Biophys. J.* 84:2852–2870.
19. Stagner, J. I., E. Samols, and G. C. Weir. 1980. Sustained oscillations of insulin, glucagon, and somatostatin from the isolated canine pancreas during exposure to a constant glucose concentration. *J. Clin. Invest.* 65:939–942.
20. Goodner, C. J., D. J. Koerker, J. I. Stagner, and E. Samols. 1991. In vitro pancreatic hormonal pulses are less regular and more frequent than in vivo. *Am. J. Physiol. Endocrinol. Metab.* 260:E422–E429.
21. Gilon, P., M. A. Ravier, J. C. Jonas, and J. C. Henquin. 2002. Control mechanisms of the oscillations of insulin secretion in vitro and in vivo. *Diabetes.* 51:S144–S151.
22. Westerlund, J., and P. Bergsten. 2001. Glucose metabolism and pulsatile insulin release from isolated islets. *Diabetes.* 50:1785–1790.
23. Ritzel, R. A., J. D. Veldhuis, and P. C. Butler. 2003. Glucose stimulates pulsatile insulin secretion from human pancreatic islets by increasing secretory burst mass: dose-response relationships. *J. Clin. Endocrinol. Metab.* 88:742–747.
24. Berman, N., H. F. Chou, A. Berman, and E. Ipp. 1993. A mathematical model of oscillatory insulin secretion. *Am. J. Physiol.* 264:R839–R851.
25. Sha, L., J. Westerlund, J. H. Szurszewski, and P. Bergsten. 2001. Amplitude modulation of pulsatile insulin secretion by intrapancreatic ganglion neurons. *Diabetes.* 50:51–55.
26. Lang, D. A., D. R. Matthews, J. Peto, and R. C. Turner. 1979. Cyclic oscillations of basal plasma glucose and insulin concentrations in human beings. *N. Engl. J. Med.* 301:1023–1027.
27. Goodner, C. J., F. G. Hom, and D. J. Koerker. 1982. Hepatic glucose production oscillates in synchrony with the islet secretory cycle in fasting rhesus monkeys. *Science.* 215:1257–1260.
28. Sturis, J., N. M. O'Meara, E. T. Shapiro, J. D. Blackman, H. Tillil, K. S. Polonsky, and E. Van Cauter. 1993. Differential effects of glucose stimulation upon rapid pulses and ultradian oscillations of insulin secretion. *J. Clin. Endocrinol. Metab.* 76:895–901.
29. Mao, C. S., N. Berman, K. Roberts, and E. Ipp. 1999. Glucose entrainment of high-frequency plasma insulin oscillations in control and type 2 diabetic subjects. *Diabetes.* 48:714–721.
30. Pørksen, N., C. Juhl, M. Hollingdal, S. M. Pincus, J. Sturis, J. D. Veldhuis, and O. Schmitz. 2000. Concordant induction of rapid in vivo pulsatile insulin secretion by recurrent punctuated glucose infusions. *Am. J. Physiol. Endocrinol. Metab.* 278:E162–E170.
31. Sturis, J., E. Van Cauter, J. D. Blackman, and K. S. Polonsky. 1991. Entrainment of pulsatile insulin secretion by oscillatory glucose infusion. *J. Clin. Invest.* 87:439–445.
32. Luciani, D. S. 2004. Oscillations of cytosolic Ca^{2+} and metabolism studied in murine pancreatic islets. Ph.D. thesis. Department of Physics, The Technical University of Denmark, Kgs. Lyngby, Denmark.
33. Hollingdal, M., C. B. Juhl, S. M. Pincus, J. Sturis, J. D. Veldhuis, K. S. Polonsky, N. Pørksen, and O. Schmitz. 2000. Failure of physiological plasma glucose excursions to entrain high-frequency pulsatile insulin secretion in type 2 diabetes. *Diabetes.* 49:1334–1340.
34. Sturis, J., C. Knudsen, N. M. O'Meara, J. S. Thomsen, E. Mosekilde, E. Van Cauter, and K. S. Polonsky. 1995. Phase-locking regions in a forced model of slow insulin and glucose oscillations. *Chaos.* 5:193–199.
35. Song, H. S., S. S. McIntyre, H. Shah, J. D. Veldhuis, P. C. Hayes, and P. C. Butler. 2000. Direct measurement of pulsatile insulin secretion from the portal vein in human subjects. *J. Clin. Endocrinol. Metab.* 85:4491–4499.
36. Bertram, R., and A. Sherman. 2004. A calcium-based phantom bursting model for pancreatic islets. *Bull. Math. Biol.* 66:1313–1344.
37. Smolen, P. 1995. A model for glycolytic oscillations based on skeletal muscle phosphofructokinase kinetics. *J. Theor. Biol.* 174:137–148.
38. Westermark, P. O., and A. Lansner. 2003. A model of phosphofructokinase and glycolytic oscillations in the pancreatic β-cell. *Biophys. J.* 85:126–139.
39. Maki, L. W., and J. Keizer. 1995. Analysis of possible mechanisms for in vitro oscillations of insulin secretion. *Am. J. Physiol. Cell Physiol.* 268:C780–C791.

40. Matschinsky, F. M., B. Glaser, and M. A. Magnuson. 1998. Pancreatic β-cell glucokinase: closing the gap between theoretical concepts and experimental realities. *Diabetes*. 47:307–315.

41. Magnus, G., and J. Keizer. 1998. Model of β-cell mitochondrial calcium handling and electrical activity. I. Cytoplasmic variables. *Am. J. Physiol. Cell Physiol.* 274:C1158–C1173.

42. Keizer, J., and G. Magnus. 1989. ATP-sensitive potassium channel and bursting in the pancreatic β-cell. A theoretical study. *Biophys. J.* 56: 229–242.

43. Bertram, R., J. Previte, A. Sherman, T. A. Kinard, and L. S. Satin. 2000. The phantom burster model for pancreatic β-cells. *Biophys. J.* 79:2880–2892.

44. Jonas, J. C., P. Gilon, and J. C. Henquin. 1998. Temporal and quantitative correlation between insulin secretion and stably elevated or oscillatory cytoplasmic Ca^{2+} in Mouse pancreatic β-cells. *Diabetes*. 47:1266–1273.

45. Henquin, J. C. 2000. Triggering and amplifying pathways of regulation of insulin secretion by glucose. *Diabetes*. 49:1751–1760.

46. Prentki, M., and F. M. Matschinsky. 1987. Ca^{2+}, cAMP, and phospholipid-derived messengers in coupling mechanisms of insulin secretion. *Physiol. Rev.* 67:1185–1248.

47. Ermentrout, G. B. 2002. Simulating, Analyzing, and Animating Dynamical Systems: A Guide to XPPAUT for Researchers and Students. SIAM Books, Philadelphia, PA.

48. Meissner, H. P. 1976. Electrophysiological evidence for coupling between β-cells of pancreatic islets. *Nature*. 262:502–504.

49. Eddlestone, G. T., A. Goncalves, and J. A. Bangham. 1984. Electrical coupling between cells in islets of Langerhans from Mouse. *J. Membr. Biol.* 77:1–14.

50. Santos, R. M., L. M. Rosario, A. Nadal, J. Garcia-Sancho, B. Soria, and M. Valdeolmillos. 1991. Widespread synchronous $[Ca^{2+}]_i$ oscillations due to bursting electrical activity in single pancreatic islets. *Pflugers Arch.* 418:417–422.

51. Valdeolmillos, M., A. Gomis, and J. V. Sanchez-Andres. 1996. In vivo synchronous membrane potential oscillations in Mouse pancreatic β-cells: lack of co-ordination between islets. *J. Physiol.* 493:9–18.

52. Jung, S. K., L. M. Kauri, W. J. Qian, and R. T. Kennedy. 2000. Correlated oscillations in glucose consumption, oxygen consumption, and intracellular free Ca^{2+} in single islets of Langerhans. *J. Biol. Chem.* 275:6642–6650.

53. Sherman, A., and J. Rinzel. 1991. Model for synchronization of pancreatic β-cells by gap junction coupling. *Biophys. J.* 59:547–559.

54. Sturis, J., K. S. Polonsky, E. Mosekilde, and E. Van Cauter. 1991. Computer model for mechanisms underlying ultradian oscillations of insulin and glucose. *Am. J. Physiol.* 260:E801–E809.

55. Barbosa, R. M., A. M. Silva, A. R. Tomé, J. A. Stamford, R. M. Santos, and L. M. Rosário. 1996. Real time electrochemical detection of 5-HT/insulin secretion from single pancreatic islets: effect of glucose and K^+ depolarization. *Biochem. Biophys. Res. Commun.* 228:100–104.

56. Barbosa, R. M., A. M. Silva, A. R. Tomé, J. A. Stamford, R. M. Santos, and L. M. Rosário. 1998. Control of pulsatile 5-HT/insulin secretion from single mouse pancreatic islets by intracellular calcium dynamics. *J. Physiol.* 510:135–143.

57. Pørksen, N., B. Nyholm, J. D. Veldhuis, P. C. Butler, and O. Schmitz. 1997. In humans at least 75% of insulin secretion arises from punctuated insulin secretory bursts. *Am. J. Physiol. Endocrinol. Metab.* 273:E908–E914.

58. Pørksen, N., T. Grofte, J. Greisen, A. Mengel, C. Juhl, J. D. Veldhuis, O. Schmitz, M. Rossle, and H. Vilstrup. 2002. Human insulin release processes measured by intraportal sampling. *Am. J. Physiol. Endocrinol. Metab.* 282:E695–E702.

59. Song, S. H., L. Kjems, R. Ritze, S. M. McIntyre, M. L. Johnson, J. D. Veldhuis, and P. C. Butler. 2002. Pulsatile insulin secretion by human pancreatic islets. *J. Clin. Endocrinol. Metab.* 87:213–221.

60. Goodner, C. J., I. R. Sweet, and H. C. Harrison, Jr. 1988. Rapid reduction and return of surface insulin receptors after exposure to brief pulses of insulin in perfused Rat hepatocytes. *Diabetes*. 37:1316–1323.

61. Sedaghat, A. R., A. Sherman, and M. J. Quon. 2002. A mathematical model of metabolic insulin signaling pathways. *Am. J. Physiol. Endocrinol. Metab.* 283:E1084–E1101.